

Towards sub-30nm Contacted Gate Pitch, Forked Contact and Dynamically-Doped Nanosheets to Enhance Si and 2D Materials Device Scaling

Aryan Afzalian, Zubair Ahmed and Julien Ryckaert
imec, Leuven, Belgium, aryan.afzalian@imec.be

Abstract

We propose a novel Forked-Contacts, Dynamically-Doped Multigate transistor as ultimate scaling booster for both Si and 2D materials in aggressively-scaled nanosheet devices. Using accurate dissipative DFT-NEGF atomistic-simulation fundamentals and cell layout extrinsics, we demonstrate superior and optimal device characteristics and inverter energy - delays down to sub-30-nm pitches, i.e., a 10 nm scaling boost compared to the nanosheet MOSFET references. **Keywords:** CMOS, CGP scaling, Si, TMD, 2d materials, dynamic-doping

Introduction

The Dynamically-Doped (D2) Field-Effect Transistor is a novel device architecture that scales better than its MOSFET nanosheet (NS) counterpart [1], owing to the suppression of ungated extensions (spacers) from the device Contacted Gate-pitch (CGP) equation [1,2] and Fig. 1a. What used to be the NS chemically doped extensions are now electrically and dynamically-doped by the gate, i.e., a part of the channel. Hence, for a given CGP, the channel length L in the D2FET is twice the spacer length (L_{SPACER}) longer than L of a standard MOSFET, as it benefits from the full distance between the source (S) and drain (D) contact pads. The gate length L_G value could even be larger than L , if the gate would overlap over the contact region of length L_C (Fig. 1). For a single-gate (SG) single-sheet device, this can simply be enabled by having the gate contact on the side opposite to the contacts, i.e., using for instance a top-contact and an individually back-gated transistor [1]. To enable a D2 tri-gate with stacked sheets, however, we propose here a doubled forked structure (E2), where the sheets are connected to a forked gate on one side and to forked S & D contacts on the other side (Fig. 1). Our simulation results show, as expected, that such a multigate E2D2 architecture enables a better electrostatic control and improved drive current at scaled CGP, especially for Si where the film thickness can be relaxed, compared to the SG-D2 transistor. We report here on the impact of the multigate E2D2 architecture innovation on intrinsic-device and loaded-inverter performance, when pitch is scaled well below 30 nm using accurate dissipative DFT-NEGF atomistic-simulation fundamentals and cell-layout extrinsics. The E2D2 architecture is benchmarked to NS MOSFETs using both Si and 2 emerging 2D transition metal dichalcogenide (TMD) monolayer (1ML) materials – one, WS_2 , with predicted fundamental drive similar to that of Si, the other, HfS_2 , featuring an enhanced fundamental drive current [1] – as test vehicles.

Methods

Current – Voltage ($I_D(V_G)$, Fig. 2d inset) and intrinsic device capacitances (C_{Gi}) (Fig. 2b) for Si and 2D TMD E2D2 and standard NS references are simulated using our first-principle

atomistic NEGF solver ATOMOS, including electron-phonon scattering [1,2]. From these simulations the intrinsic single-sheet device fundamental performance vs. CGP can be assessed (Fig. 2). For each CGP, a full device optimization is made including film thickness (t_s) scaling for Si and extension doping for the NS. Note that the detrimental impact of quantum confinement, including mobility degradation, and source-to-drain direct tunneling are naturally included in our quantum transport solver. For computing stacked-inverter energy-delay products (Fig. 3), the extracted extrinsic capacitance of the cell layout C_{cell} and the backend-of-line load, C_{BK} are used (Fig. 1). C_{cell} values are reported in Fig. 4a. The number of stacked sheets (n_s) used is computed to allow a total stack height of 60 nm for all devices. n_s is the same for E2D2 and NS of a same material ($n_s = 4$ for Si and 5 for the TMDs owing to their 1ML thickness of about 0.6 nm [1]). The available width for a single sheet, W , in our 5-track E2D2 layout cell is 12 nm. The standard NS layout is described in [3] and W is 12 nm as well.

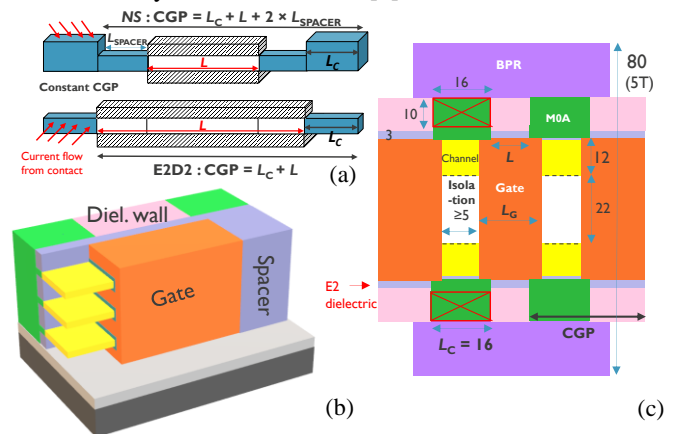


Fig. 1 E2D2 device structure. a) Side view schematic of a single-sheet multigate conventional NS (Top) and E2D2 transistor (Bottom) with same CGP. b) 3D view showing the doubled forked (E2) structure, c) cell layout of the 5-track (cell height = 80 nm) E2D2 inverter cell with buried power rail (BPR). The technological dimensions, we assumed for this study are indicated in the figure. We assumed $L_G = L$. $L_C = 16$ nm, $L_{\text{SPACER}} = 5$ nm. The width of an individual sheet is $W = 12$ nm. The P/N separation is 22nm. For the gate oxide, we assumed a 2 nm hafnium oxide with $\epsilon_R = 15.6$. The gate stack metal thickness is 6 nm. The channel (white region in Fig. 1a) is intrinsic. The contact regions (in blue in Fig. 1a) are doped. $n_s = 4$ for Si and 5 for 2D.

Results

Owing to its 10 nm extended gate length at same CGP, the E2D2 SS and, hence, I_{ON} at fixed I_{OFF} are superior compared to that of the NS as CGP is scaled below 30 nm for all materials. The E2D2 C_{Gi} are however larger at fixed CGP, the net effect being that the **E2D2 optimal intrinsic delay is comparable to that of its NS counterpart, but shifted towards smaller**

CGPs by about 10 nm, i.e., $2 \times L_{\text{SPACER}}$ (Fig. 2). Hence the E2D2 architecture enables a significant scaling boost. For Si, the optimal NS and E2D2 delays are obtained at CGP = 36, and 26 nm, respectively, i.e., $L_G = 10$ nm and $t_s = 3$ nm in both cases. For the 2D materials, a further 5 nm scaling boost is observed, and optimal delays are achieved at CGP = 31 and 21 nm for the NS and E2D2 respectively, corresponding to $L_G = 5$ nm in both cases. For the TMDs the 21 nm E2D2 CGP corresponds to the case where CGP is only limited by the contacts (L_C and the minimum isolation spacing, IS, required to separate subsequent pads, assuming $IS = L_{\text{SPACER}}$ (Fig. 1)), hence ultimate gate scaling has been achieved. Further CGP reduction could only be achieved by scaling the contacts.

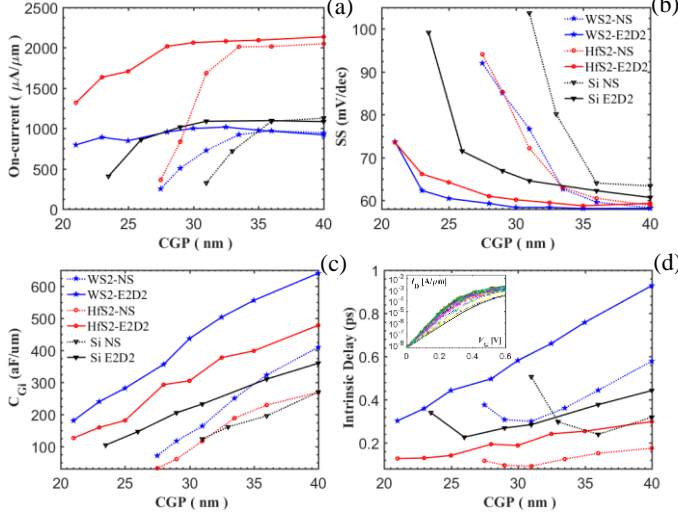


Fig. 2 a) On-current (I_{ON}) at fixed I_{OFF} , b) subthreshold slope (SS), c) intrinsic gate capacitance (C_{Gi}) and d) intrinsic delay - assuming an effective current $i_{\text{eff}} = 0.45 \times I_{\text{ON}}$ - vs. CGP for Si and for WS₂ and HfS₂ 2D monolayers NS and E2D2 architectures from ab-initio - NEGF transport simulations (the trace of the $I_{\text{D}}(V_{\text{G}})$ characteristics are in the inset) [1]. For the NS, $L_G = \text{CGP} - L_C - 2 \times L_{\text{SPACER}}$, while for E2D2 $L_G = \text{CGP} - L_C$. $L_C = 16$ nm, $L_{\text{SPACER}} = 5$ nm. I_{ON} is normalized by the gate perimeter. $I_{\text{OFF}} = 5$ nA/ μm . $V_{\text{DD}} = 0.6$ V.

Next, we investigate the switching energy vs. delay (EDP) of high-performance stacked E2D2 and NS loaded inverters for different CGPs at various V_{DD} (Fig. 3). For HfS₂ E2D2 and NS invertors, the optimal EDP is achieved at CGP = 21, $L_G = 5$ nm and CGP = 31, $L_G = 5$ nm respectively. We obtain a similar result for the WS₂ case (not shown here). For Si E2D2 and NS invertors, the optimal EDP is achieved at CGP = 26, $L_G = 10$ nm and CGP = 36, $L_G = 10$ nm respectively. Any further attempt to scale CGP by scaling L_G beyond this optimal value results in significant performance reduction (for the TMD E2D2 it is simply not possible to further scale CGP with L_G scaling). **These results further confirm the 10 nm improved scalability, we obtained from the intrinsic device performance and delays (Fig. 2). The E2D2-invertor improved EDP performance compared to that of the NS is mostly linked to the reduced C_{BK} owing to CGP scaling.**

This is confirmed in Fig. 4, where the loaded-invertor EDPs are shown for the 3 material cases at their optimal CGP and L_G values with and without C_{BK} included in the load. Regardless

of the material system used, without C_{BK} (Fig. 4.a), the E2D2 performance are similar to that of their NS counterparts, while they are enhanced when C_{BK} is included (Fig. 4.b) (the E2D2 and NS devices also share the same optimal L_G of 10 nm for Si and 5 nm for the TMDs).

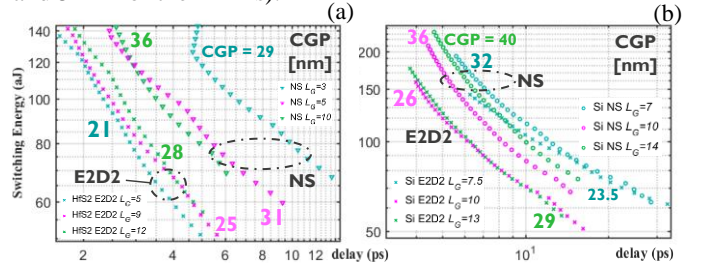


Fig. 3 Switching energy vs. delay (EDP) of high-performance stacked E2D2 and NS inverter cells for different CGP and L_G , as indicated in the figures, at various V_{DD} (0.4V to 0.7V). The devices are made of a) 1ML-HfS₂ with $n_s = 5$ sheets/device, b) Si with $n_s = 4$ sheets/device and optimized Si thickness t_s ranging from 3 to 5 nm. The invertors are loaded with the extrinsic capacitances of the cell layout C_{Cell} and a 50 CGP-long metal line with capacitance $C_{\text{BK}} = 198$ aF/ μm [4]. $I_{\text{OFF}} = 5$ nA/ μm .

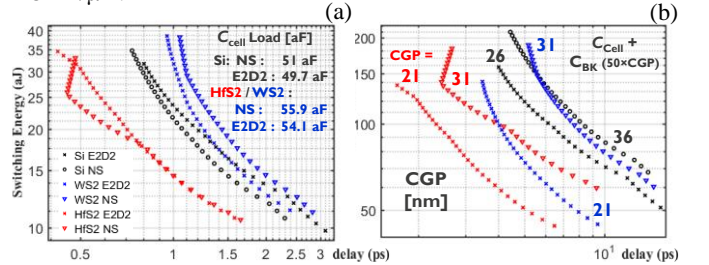


Fig. 4 EDP of the Si, WS₂ and HfS₂ stacked E2D2 and NS inverter cells at optimal CGP as indicated in Fig. 4b, at various V_{DD} (0.4V to 0.7V). The invertors are loaded with a) C_{Cell} only, its value for each inverter case is indicated in the figure, b) C_{Cell} and a 50 CGP-long metal line C_{BK} . $I_{\text{OFF}} = 5$ nA/ μm .

Conclusions

We proposed a compact E2D2 multigate architecture that enables sub-30-nm CGP, i.e., an improved $2 \times L_{\text{SPACER}}$ pitch scaling, compared to a NS reference, owing to the suppression of ungated extensions from the CGP equation. This E2D2 scaling benefits were measured in term of similar intrinsic performance and optimal delay but at a 10 nm reduced CGP. A similar conclusion was found comparing E2D2 and NS stacked-invertor cells. For backend-loaded invertors, the E2D2 EDP performance is further enhanced due to CGP and, hence, C_{BK} reduction. Similar relative benefits were observed regardless of the material system used. Compared to Si, a mature 2D material technology could potentially further enable an extra 5-nm CGP scaling boost, both for the E2D2 and NS architectures, with same or improved performance, if respectively WS₂, a material with a fundamental drive similar to Si, or HfS₂, a higher mobility material, were used.

References

- [1] A. Afzalian, *npj 2D Mater Appl* **5**, 5 (2021).
- [2] A. Afzalian, *IEEE Trans Electron Devices*, **68**, 11, 2021.
- [3] Z. Ahmed, *IEDM*, 2020, pp. 22.5.1.
- [4] <https://irds.ieee.org/editions/2018>